AAPS PharmSciTech, Vol. 10, No. 4, December 2009 (© 2009)
DOI: 10.1208/s12249-009-9328-9

Research Article

Microemulsion System with Improved Loading of Piroxicam: A Study of Microstructure

Muhammad Faizan Nazar,[1] Asad Muhammad Khan,[1,2,3,4] and Syed Sakhawat Shah[1,4]

Received 22 July 2009; accepted 13 October 2009; published online 30 October 2009

Abstract. Formulation of a new oil-in-water (*o*/*w*) microemulsion composed of castor oil/Tween 80/ethanol/phosphate buffer for enhancing the loading capacity of an anti-inflammatory drug piroxicam has been accomplished. The pseudo-ternary phase diagram has been delineated at constant surfactant/cosurfactant ratio (1:2). The internal structure of so created four-component system was elucidated by means of an analysis of isotropic area magnitudes in the phase diagram. Conductivity (σ), kinematic viscosity (k_η), and surface tension (γ) studies with the variation in Φ_w (weight fraction of aqueous phase) show the occurrence of structural changes from water-in-oil (*w*/*o*) microemulsion to oil-in-water (*o*/*w*). Along with the solubility and partition studies of piroxicam in microemulsion components, the changes in the microstructure of the microemulsion after incorporation of drug have been evaluated using pH, σ, γ, k_η, and density studies. Piroxicam, a poorly water-soluble drug displayed high solubility (1.0%) in an optimum microemulsion formulation using ethanol (55.0%), Tween 80 (26.5%), castor oil (7.5%), and phosphate buffer (11.0%). The results have shown that the microemulsion remained stable after the incorporation of piroxicam. Fluorescence spectra analysis taking pyrene as fluorescent probe was performed, and the results showed that pyrene was completely solubilized in the oil phases of the bicontinuous microemulsions. The fluorescence spectrum of the model drug piroxicam was used to probe the intramicellar region of nonionic microemulsion. The results showed that the piroxicam was localized in the interfacial film of microemulsion systems more deeply in the palisade layer with ethanol as the cosurfactant.

KEY WORDS: isotropic area; microemulsion; piroxicam; spectroscopy; structural changes.

INTRODUCTION

Piroxicam is a nonsteroid anti-inflammatory compound with analgesic and antipyretic effects, used for the treatment of rheumatoid arthritis, osteoarthritis, and traumatic contusions. However, it has been associated with gastrointestinal side effects. It is possible to minimize these problems by developing drug carriers to prevent the direct contact of drug with gastric mucosal or that allow the topical administration of drug (1,2).

Microemulsions are optically isotropic, transparent, and thermodynamically stable homogeneous solutions of oil and water, stabilized by addition of a surfactant and usually a cosurfactant (3,4). These structures have been considerably investigated as drug delivery and carrier system for a wide range of drugs, including analgesics and anti-inflammatory, and also used to dissolve lipophilic drugs in aqueous medium or hydrophilic drugs in lipophilic medium (4,5). Oil-in-water microemulsions have been described as a reservoir system that can inhibit drug release, increasing the topical effect (6). Several mechanisms have been proposed to explain the advantages of microemulsion or the transdermal delivery of drugs (7). First, a large amount of drug can be incorporated in the formulation due to the high solubilizing capacity, with increased thermodynamic activity toward the skin. Second, the permeation rate of a drug from microemulsion may be increased, since the affinity of the drug to the internal phase in microemulsion can be easily modified, to favor partitioning, using different internal phases and changing the composition of the microemulsion. Third, the surfactant and cosurfactant used in the microemulsion may reduce the various diffusional barriers by acting as penetration enhancers (8,9).

For the selection of components of a biocompatible microemulsion system, the use of nonionic surfactants has been widely accepted, since these are compatible and retain its utility over a broad range of pH values and may affect the skin barrier function (10–12).

Microemulsion comprises different structures (water-in-oil (*w*/*o*), oil-in-water (*o*/*w*), and bicontinuous) and these help in releasing the drug (13,14). It is necessary to characterize the microstructure of pure and drug-loaded microemulsion. The changes in the internal structure of a microemulsion can

[1] Department of Chemistry, Quaid-i-Azam University, 45320 Islamabad, Pakistan.
[2] Department of Chemistry, Forman Christian College (A Chartered University), 54600 Lahore, Pakistan.
[3] School of Science and Engineering, LUMS, Opposite U Block, DHA, 54792 Lahore, Pakistan.
[4] To whom correspondence should be addressed. (e-mail: amk.qau@gmail.com); (e-mail: ssshah.qau@gmail.com)

be monitored by analyzing conductivity, viscosity, density, surface tension, the fluorescence probe studies, *etc*. (15–17). The incorporated drug may or may not influence the microstructure. *o*/*w* and *w*/*o* microemulsions may show different behavior for the release of both hydrophilic and lipophilic drugs.

In the present work, an attempt has been made to construct a microemulsion system for poorly water-soluble nonsteroid anti-inflammatory drug piroxicam, comprising of castor oil, a nonionic surfactant Tween 80, a short-chain alkanol cosurfactant (ethanol), and phosphate buffer (PB) pH 7.4. The pseudo-ternary phase diagram has been constructed for the chosen system at a constant surfactant/cosurfactant ratio (1:2). The reason for the selection of the particular oil chosen was that the castor oil has a hydroxyl group in addition to unsaturation, making it more polar. Ricinoleic acid is the main component of castor oil and it exerts anti-inflammatory effects (18). Polyoxyethylene fatty acid, stearic acid, and oleic acid are used in emulsifiers in oil/water type creams and lotions.

Conductivity, viscosity, surface tension, and the fluorescence behavior of the pyrene are employed to investigate the gradual changes occurring in the microstructure of microemulsion. Pyrene is popular fluorescent probe, which is used to study the microheterogeneous media. The fluorescence spectrum of pyrene was used to sense the micropolarity of the *o*/*w* microemulsion. In addition, how stability, optical texture, and microstructure of microemulsion formulation are influenced by piroxicam is analyzed. To improve the solubility of piroxicam, an effort has been made to develop an optimum *o*/*w* microemulsion. It is therefore expected that the use of microemulsion formulation may enhance the solubility of piroxicam and prevent its degradation.

MATERIALS AND METHODS

Materials

Tween 80 (polyoxyethylene sorbitan monooleate), absolute ethanol (≥99.8%), and castor oil were purchased from Fluka. Pyrene (98%) was purchased from Sigma-Aldrich.

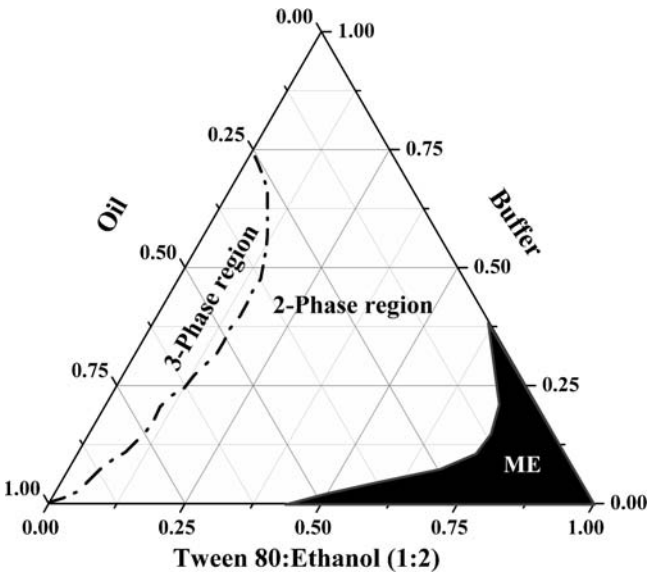

Fig. 1. Pseudo-ternary phase diagram showing microemulsion region of Tween 80/ethanol/castor oil/buffer at 25°C

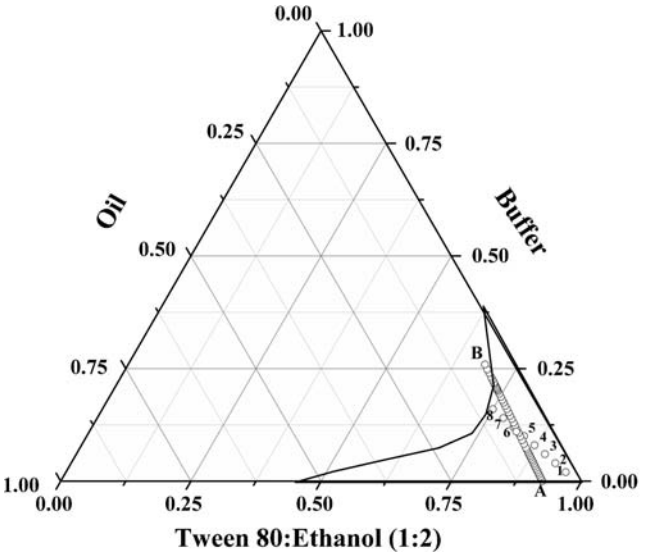

Fig. 2. Pseudo-ternary phase diagram showing microemulsion region of Tween 80/ethanol/castor oil/buffer at 25°C. *AB* represents the dilution line, and compositions *1–8* were selected for further investigations

Piroxicam was generously provided by Amson Vaccines & Pharma (PVT) Ltd and used without further purification. Phosphate buffer (0.01 M, pH 7.4) was used as the hydrophilic phase. Buffers were prepared using NaH_2PO_4/Na_2HPO_4. 0.1 M NaOH and HCl were used to maintain the pH of the solution.

Methods

Microemulsion Preparation

The pseudo-ternary phase diagram was mapped (as shown in Fig. 1) using oil (castor oil), surfactant (Tween 80; HLB=15), cosurfactant (ethanol), and aqueous phase PB (pH 7.4) at 25± 0.01°C with constant surfactant/cosurfactant mass ratio (1:2). The temperature was kept at 25±0.01°C and was maintained by a Lauda M-20 thermostat. Castor oil was first mixed with Tween 80/ethanol mixture; PB was then added to obtain the desired microemulsion compositions. Transparent, single-phase mixtures were designated as microemulsions. All the samples were stable for over 10 months, remaining clear and transparent.

Drug Incorporation in Microemulsion

Eight microemulsions differing from each other by Φ_w were selected from the single-phase region of phase diagram (Fig. 2) with compositions mentioned in Table I to study their potential as drug delivery system. All of them show stability over 10 months and remain clear and transparent. Piroxicam was dissolved into the pre-weight oil component of the system at a concentration of 1% (*w*/*w*) under stirring followed by addition of remaining components.

Microemulsion Characterization

Optical Transparency

The homogeneity and optical isotropy of pure and drug-loaded microemulsions were examined by a Polarimeter

Table I. Selected Microemulsion Formulations (%, *w*/*w*)

	1	2	3	4	5	6	7	8	ME[a]
Castor oil	2.2	3.4	4.6	5.8	7.0	8.2	9.4	10.6	7.5
Buffer	2.0	4.0	6.0	8.0	10.0	12.0	14.0	16.0	11.0
Tween 80	32.0	30.7	29.5	28.3	27.2	26.2	25.0	23.6	26.5
Ethanol	63.8	61.8	59.9	57.8	55.7	53.6	51.6	49.8	55.0

[a] Selected microemulsion (ME) for further analysis

(ATAGO, AP-100 Automatic Polarimeter) and visual examination at room temperature.

Centrifugation

Thermodynamic stability of pure and drug-loaded microemulsions was tested by carrying out centrifugation at 5,500 rpm for 20 min using (Hermle Z200) centrifuge.

Surface Tension

Surface tension measurements were made at 25±0.01°C under atmospheric pressure by Torsion Balance (White Elec. Inst. Co. Ltd.) equipped with a ring having circumference of 4.0 cm. The experimental error was about ±0.05 mN m^{-1}.

Density and Specific Gravity

Densities and specific gravity of pure and drug-loaded microemulsions were measured by making use of an Anton Paar (Model DMA 5000) density meter at 25±0.01°C. The density meter was calibrated before and after each set of density measurement using the density of air and pure water.

Refractive Index

The refractive indices of the formulations were determined using a refractometer (ATAGO, RX-5000) by placing one drop of solution on the slide.

pH

The apparent pH of all the selected microemulsions and the drug-loaded microemulsion was determined using a pH Meter (WTW 82362 Weilheim) fitted with a pH electrode (WTW A061414035). The temperature was maintained at 25±0.01°C by a Lauda M-20 thermostat.

Conductivity Measurements

The effect of the amount of water phase of microemulsion was monitored quantitatively by measuring the electrical conductivity. The electric conductivity (σ) was measured by means of a Microprocessor Conductivity Meter (WTW 82362 Weilheim) fitted with an electrode (WTW 06140418) having a cell constant of 1.0 cm^{-1}. The temperature was kept at 25±0.01°C and was maintained by a Lauda M-20 thermostat. Conductivity measurements were carried out by titration of oil, surfactant/cosurfactant mixture with buffer (along the dilution line *AB* in Fig. 1). Further the conductivity of selected and drug-loaded microemulsions was also measured. The error limit of conductance measurements was ±0.02 μ**S** cm^{-1}.

Viscosity Measurements

Viscosities were measured with calibrated Ubbelhode viscometer at 25±0.1°C. For each measurement, the viscometer was washed, rinsed, and vacuum-dried. To follow the viscous behavior of the microemulsions, flow time was measured for all the selected and drug-loaded microemulsions (1 wt.% drug). The error limit of viscosities measurements was ±3%.

Absorption and Steady-State Emission Measurements

The absorption and steady-state fluorescence spectra were recorded using a Perkin Elmer Lambda 20 spectrophotometer and a Perkin Elmer LS 55 luminescence spectrometer, respectively, both with an external temperature controlled cell holder at a temperature of 25.0±0.1°C. The fluorescence emission spectrum of pyrene (excitation at 340 nm) was used to obtain the ratio of intensities of the first to the third vibronic peaks (I_1/I_3). Good resolution of the bands was obtained at the slit width (ex. 5.0 nm, em. 5.0 nm). The scan range used was from 350 to 500 nm. The Photo Multiplier tube voltage was kept at 665 V. The concentration of pyrene was 1.0 μM. The intensities for I_1 and I_3 are taken at 373 and 384 nm, respectively. The fluorescence emission spectrum of piroxicam at λ_{exc} 370 nm was obtained where the emission and excitation slits were fixed at 7.0 nm. The scan range used was from 390 to 650 nm. The concentration of piroxicam was 10.0 μM.

To quantify the solubilization of piroxicam in micellar media of Tween 80–ethanol system, differential absorbance measurements were made in such a way that drug (piroxicam) solution of a particular concentration (1.0×10^{-5} M) was kept on reference side and the Tween 80–ethanol–piroxicam solution on the sample side in the spectrophotometer.

Partition Coefficients

Oil/buffer partition coefficient was determined by dissolving 20 mg piroxicam in 2 mL castor oil. Buffer was added in 1:1 ratio (*v*/*v*). The mixture was shaken for 10 min and centrifuged for 2 h. The two layers were separated and the content of piroxicam in aqueous layer (PB) was assayed by UV–Visible spectrophotometer at 371 nm. The final content of drug in the lipophilic phase was calculated by subtracting the content of piroxicam in aqueous phase from initial loaded content of drug in the lipophilic phase. Further, the effect of the presence of Tween 80 and ethanol on the partition of

Table II. Physical Parameters of Selected Microemulsion (ME) and After Incorporation of Drug

	S/CoS=1:2	
Physical property	Value (no drug)	Value (drug-loaded)
Refractive index	1.40053	1.40345
Conductivity (μs/cm)	4.65	4.60
Kinematic viscosity (cP L g^{-1})	13.05	14.90
Density (g L^{-1})	0.92949	0.93572
Viscosity (cP)	12.13	13.94
Surface tension (mN/m)	30.4	30.6
specific Gravity	0.93225	0.93850
pH	6.05	5.50

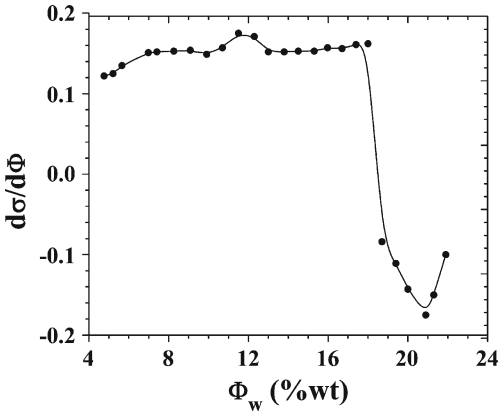

Fig. 4. The first derivative of the electric conductivity $d\sigma/d\Phi_w$ as a function of weight fraction of aqueous phase (Φ_w)

piroxicam in oil/buffer was studied by adding 5% (*w*/*v*) of each Tween 80 and ethanol.

RESULTS AND DISCUSSION

In the present system, microemulsion was prepared using castor oil (fatty acid), which induces highly permeable pathways in the stratum corneum (18–20). Tween 80 is a widely accepted nonionic surfactant, used in many pharmaceutical formulations (21–23). The cosurfactant (ethanol) is used to study the one phase microemulsion region. The presence of alcohol overcomes the need for any additional input of energy. These properties make the components useful as vehicles for drug delivery (24–26).

In the absence of aqueous phase, a solution-like oily phase consisting only of surfactant, oil, and ethanol exists. Ethanol interacts with the ethoxylated head groups of the Tween 80 by hydrogen bonding and affects its critical packing parameter. When water is progressively added to the concentrate it facilitates the organization of the hydrated head groups of the surfactant into a polar core, while the fatty acid tails are immersed in the oil continuous phase. The ethanol suppresses formation of lyotropic liquid crystals. Any free aqueous phase is entrapped in the microstructures. Thus, *w*/*o* microstructures are formed. Upon further dilution, the reversed nanostructures grow and convert into a bicontinuous phase and finally invert into *o*/*w* microstructures without phase separation.

Phase Studies

Figure 1 shows the pseudo-ternary phase diagram and area of existence of microemulsion for Tween 80/ethanol/castor oil/phosphate buffer. Microemulsion in the present study formed spontaneously at ambient temperature when their components were brought in contact.

Phase behavior investigations of this system demonstrated the suitable approach of determining the water phase, oil phase, surfactant concentration, and cosurfactant concentration with which the transparent, one-phase, low-viscous microemulsion system was formed. The phase behavior, as shown by Fig. 1, manifests a two-phase region, a three-phase region, and a large single-phase region, which gradually and continuously transformed from buffer-rich side of binary solution (buffer/surfactant micellar phase) of pseudo-ternary phase diagram toward the oil-rich region. This stresses a continuous transition from water-rich compositions to oil swollen micelles.

The phase study revealed that the maximum proportion of oil was incorporated in microemulsion systems when the surfactant-to-cosurfactant ratio was 1:2. From a formulation viewpoint, the increased oil content in microemulsions may provide a greater opportunity for the solubilization of piroxicam. Eight microemulsions (1–8) were selected from the single-phase isotropic region (Fig. 2), with compositions mentioned in Table I. Selected microemulsion (ME) was further analyzed by conductivity, viscosity, density, surface tension, refractive index, and pH. The values of measured parameters have been presented in Table II.

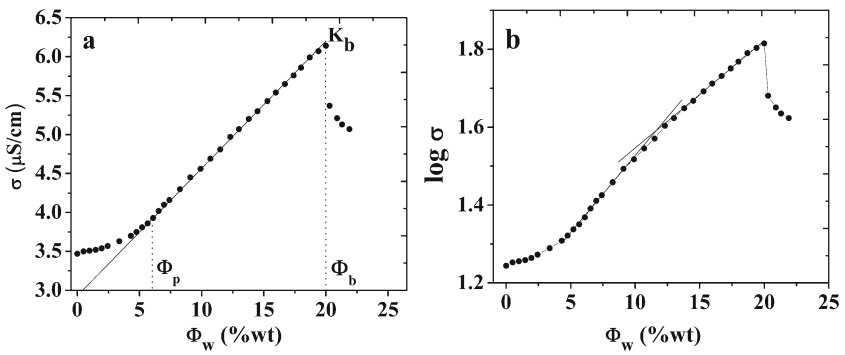

Fig. 3. Variation of σ (**a**) and log σ (**b**) of four-component microemulsion system with Φ_w (wt.%) along the dilution line *AB* (as shown in Fig. 2)

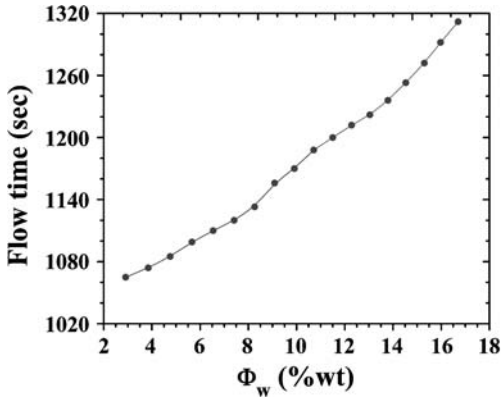

Fig. 5. Efflux time of oil, surfactant/cosurfactant mixture as a function of weight fraction of aqueous phase (Φ_w)

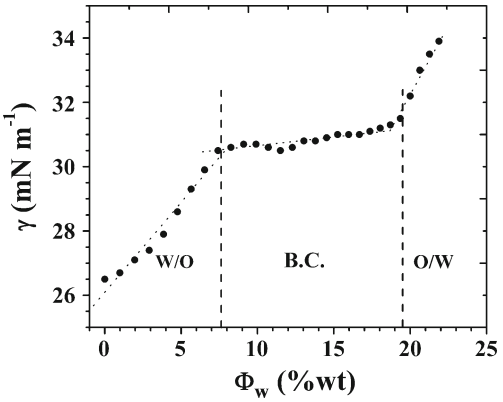

Fig. 7. Variation of surface tension with the weight fraction of aqueous phase (Φ_w)

Conductivity Measurements

Conductometry is a useful tool to assess microemulsion structure. Conductivity studies have explained the existence of a characteristic zone with an isotropic microemulsion domain in a continuum. For the determination of electric conductivity (σ) as a function of weight fraction of aqueous component Φ_w (wt.%) for the oil, surfactant/cosurfactant mixture along the dilution line AB (shown in Fig. 2) has been carried out. The results of variation of σ *versus* Φ_w (wt.%) are shown in Fig. 3a. The behavior exhibits profile characteristic of percolative conductivity (27–29). The conductivity is initially low in an oil–surfactant mixture but increases with increase in aqueous phase.

As the volume fraction of water increases, the electrical conductivity of the system slightly increases as well, until the critical Φ_w is reached. At this stage, a sudden increase in conductivity is observed. This phenomenon is known as percolation, and the critical Φ_w at which it occurs is known as percolation threshold Φ_p (27).

The value of conductivity below Φ_p suggests that the reverse droplets are discrete (forming *w*/*o* microemulsion) and have little interaction. Above Φ_p the value of σ increases linearly and steeply till it touches the value of K_b. The interaction between the aqueous domains becomes progressively more important and forms a network of conductive channel (bicontinuous microemulsion) (30).

Rapid increase in conductivity beyond the percolation threshold ($\Phi_p \approx 6\%$) up to approximate value of 20% of Φ_w indicates the existence of network of conductive channels, which corresponds to the formation of water cylinders or channels in an oil phase due to the attractive interactions between the spherical microdroplets of water phase in the *w*/*o* microemulsion.

Increasing water content above Φ_b (Φ_w>20%), the σ shows a dip in the measured values, which may be due to strong attractive forces as system becomes more viscous (16,30). Figure 3b depicts the variation of log σ *versus* weight fraction of water (Φ_w). The change in the slope of log σ can be attributed to the structural transition to bicontinuous from *w*/*o* (23), nearly at Φ_w=6%. The transition takes place once the aqueous phase becomes continuous phase, i.e., at Φ_b. This is in line with the observation made in phase study. Figure 3a illustrates occurrence of three different structures (namely *w*/*o*, bicontinuous, *o*/*w*). The conductivity of the microemulsions containing more than 20 wt.% water decreased significantly, probably due to the higher viscosity.

The percolation threshold can be determined from the plot ($d\sigma/d\Phi_w$), as a function of the water weight fraction, Φ_w (wt.%) (30). A maximum in the first derivative of conductance Φ_w at ~12 wt.% water is observed (Fig. 4), confirming the presence of percolation behavior (bicontinuous microstructure) in this region (31). The electric conductivity of pure selected and drug-loaded microemulsion (1.0%) is given in Table II. A comparison of two systems shows that drug incorporation does not affect the microstructure of the microemulsion.

Viscosity Measurements

To avoid the ambiguity of non-Newtonian flow behavior of microemulsion, the flow time has been used as an index of

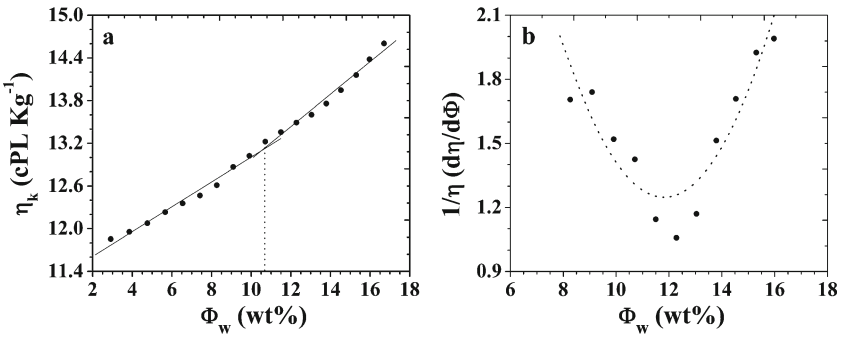

Fig. 6. Variation of kinematic viscosity (**a**) and $1/\eta\ d\eta/d\Phi_w$ (**b**) as a function of weight fraction of aqueous phase (Φ_w). *Inset* $d^2\eta/d^2\Phi_w$ as a function (Φ_w)

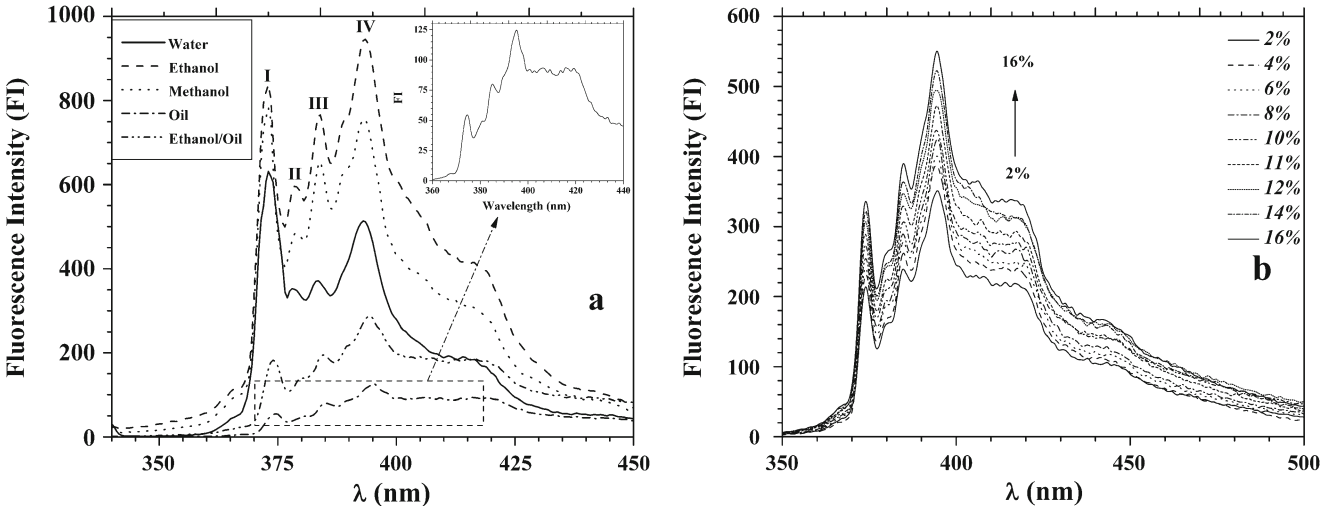

Fig. 8. The fluorescence spectra of pyrene in water, individual oil phase, in alcohols (**a**), and all the selected microemulsions (**b**)

viscosity (32). Flow time of oil, surfactant/cosurfactant mixture along the dilution line *AB*, as shown in Fig. 2, was measured as a function of weight fraction of water Φ_w (wt.%) and is shown in Fig. 5. There is a consistent increase in flow time with the increase in the Φ_w as depicted by Fig. 5. Increase in flow time can be correlated to the increasing size of the droplet.

Similar trend has been observed for the viscosity of oil, surfactant/cosurfactant mixture as a function of Φ_w (Fig. 6). The rapid change in the viscosity is probably due to the change in the microstructure of the microemulsion. The change in the internal structure could be due to either the change in the shape of droplets or may be due to the transition from *w/o* to bicontinuous microemulsion. It is well known that increase of volume fraction of dispersed phase in microemulsion increases viscosity of the system (33). For the system studied viscosity increases with increase in Φ_w (wt.% of aqueous phase).

Difference in the viscosities is more profound for lower water content values in comparison to the dilute system. The microemulsion system is turning to be more viscous with addition of water and thus may help in the slow diffusing of drug at infinite dilution. The microemulsion system thus shows a structural change from oil continuous system to water continuous, which has higher viscosities than the former (34).

The plots of k_η (kinematic viscosity), $d^2\eta/d^2\Phi_w$ and $1/\eta\ d\eta/d\Phi_w$ *versus* Φ_w reflect that the transition occurs at ~11% weight fraction of aqueous phase as shown by Fig. 6. The transition point of surface tension, conductivity, and viscosity plots coincides well at ~11% weight fraction of aqueous phase and confirms the presence of percolative behavior.

Surface Tension

Figure 7 demonstrates that the surface tension increases linearly over the same range of water content, but two breaks (at ~7.0 and ~20 wt.% water) suggest that structure changes occur at these compositions. The surface tension measurements showed increment, when measured as a function of weight fraction of aqueous component, except for the ~12% weight fraction where the value suddenly decreased and thereafter a regular increase was observed. This low surface tension value showed the presence of bicontinuous microemulsion between oil- and water-rich system, which is because of the presence of self-assembled organize microstructure in it (14,35). The results coincide well with the electric conductivity and viscosity measurements. It can be assumed that the added alcohol (ethanol) is incorporated in the interfacial structure in such a way that more water is on

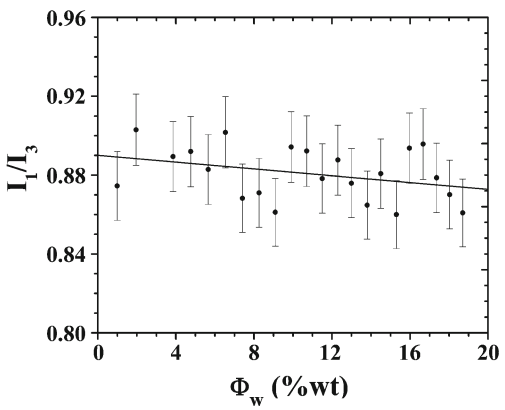

Fig. 9. Fluorescence intensity ratio (I_1/I_3) of pyrene *versus* weight fraction of aqueous phase (Φ_w)

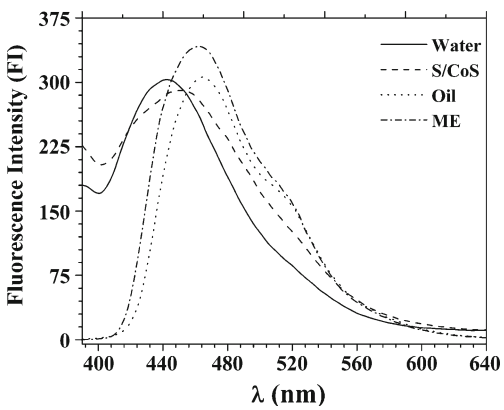

Fig. 10. The fluorescence spectra of piroxicam in water, individual oil phase, in S/CoS, and in the optimum microemulsion

Table III. Oil/Buffer Partition Coefficients (Mean ± SD)

System	Partition coefficient (p)	Log p
Oil/buffer	1.09×10^5	5.03±0.20
Oil/buffer (ethanol 5%, *w/v*)	7.26×10^4	4.86±0.15
Oil/buffer (Tween 80 5%, *w/v*)	1.35×10^3	3.13±0.20

the outside of the "oil drops", causing the increase in surface tension. Incorporation of drug showed a negligible change in the surface tension measurements, therefore indicting the possibility of piroxicam molecules into the palisade layer on the inner side of microemulsion.

Fluorescence Measurements

In the case of oil-in-water microemulsions, the steady-state fluorescence technique was successfully applied. Fluorescence measurements of the hydrophobic probe mainly depend on the polarity of the medium, and hence in bicontinuous microemulsions, it is a good indication of the polarity of the microenvironment in the microemulsion structure (36,37). The fluorescence spectra for pyrene molecule in water, individual oil phase, in alcohols (i.e., ethanol and methanol), and in ethanol/oil are shown in Fig. 8a.

There are four principal vibronic bands in the fluorescence spectrum shown in Fig. 8a and are labeled I to IV. The peak intensity ratio I_1/I_3 in the steady-state fluorescence spectra is a measurement of the relative polarity of pyrene's environment (17). Since pyrene reactant is substantially more soluble in oil phases, I_1/I_3 is expected to be lower in these phases (38). In the present work, for oil phase, the I_1/I_3 value is 0.68. In relatively polar methanol and ethanol media, I_1/I_3 values were found to be 1.20 and 1.09, respectively. Water is a highly polar solvent; the solubility of pyrene in this solvent is less than 2 μM. Hence the possibility of formation of excimer leading to I_3 signal is extremely low in water. Experimentally I_1/I_3 value is 1.70 was obtained for this medium.

Figure 8b shows the fluorescence spectra of all the compositions of microemulsion when pyrene is incorporated in their solutions. An overall increase in the intensity of all the four peaks was observed for 2% to 16% of water fraction. The reason might be that as we increase the water fraction,

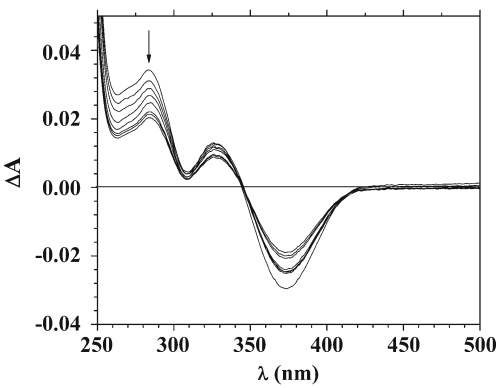

Fig. 11. Differential absorption spectra of Tween 80–ethanol–piroxicam. *Arrow* indicates the wavelength used for analysis

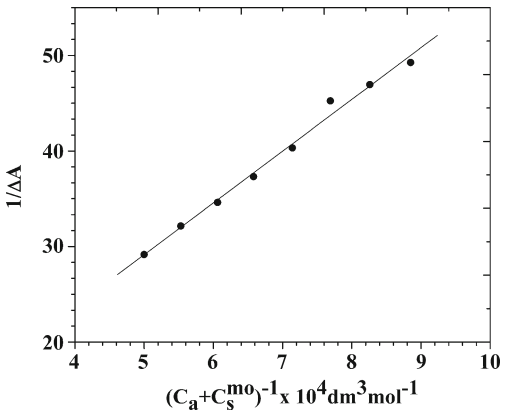

Fig. 12. Relation between $1/\Delta A$ and $(C_a+C_s^{mo})^{-1}$ for piroxicam and concentration of Tween 80

more and more pyrene is partitioned into the oil phase, and hence an increase in the fluorescence intensity is observed.

Plot of I_1/I_3 *versus* weight fraction of aqueous component composition in microemulsion is shown in Fig. 9. The value of I_1/I_3 varies between 0.85 and 0.91, which is comparable to a change from oil to water (0.68 and 1.70, respectively).

The I_1/I_3 fluorescence ratios of pyrene strongly suggest that this probe resides in microenvironments of polarity much lower (oil phase) than that of water or alcohol (39). The polarities of these microphases are similar to those of cosurfactant/oil mixtures (0.94). The following generalizations may be made regarding the fluorescence probe behavior in bicontinuous microemulsions. The I_1/I_3 values obtained by fluorescence measurements for all the stable bicontinuous microemulsions are closer to 0.88. These results suggest that pyrene is efficiently segregated from the water phase (40). The I_1/I_3 values in bicontinuous microemulsions systems are closer to the respective pure oil phase. This is due to complete solubility of pyrene in oil phases of the bicontinuous microemulsions. We conclude that all the microemulsions have separate oil microphases, in which pyrene resides.

Fluorescence Behavior of Piroxicam

The fluorescence spectra for piroxicam molecule in water, individual oil phases, in surfactant/cosurfactant mixture (1:2), and in the optimum microemulsion system are shown in Fig. 10.

For oil phase the emission maxima (λ_{em}) is 465 nm. In S/CoS (1:2) system λ_{em} is 451 nm. Water is a highly polar solvent; the solubility of piroxicam in this solvent is lower than 10 μM. The λ_{em} of piroxicam in water is 442 nm. The emission maximum in bicontinuous microemulsion system is (462 nm) closer to the respective pure oil phase. The results showed that the piroxicam was localized in the interfacial film of microemulsion systems more deeply in the palisade layer.

Table IV. Values of K_c, p, and ΔG_p° of Piroxicam in Micellar Solution of Tween 80

K_c (dm^3 mol^{-1})	p	ΔG_p° (kJ/mol)
4.2×10^3	2.33×10^5	−30.62

Partition Coefficient

Partition coefficients influence drug transport characteristics, which involve drug absorption, retention, distribution, and elimination. Since drugs are distributed by the blood, they must penetrate and traverse many cells to reach the site of action. Hence, partition coefficients will determine what tissues a given compound can reach.

Oil/Buffer Partition Coefficients

The partition coefficient (log p) of piroxicam in oil/buffer is 5.03±0.20. The presence of ethanol (5% in buffer) does not affect the partition coefficient (data shown in Table III) whereas Tween 80 (5% in buffer) reduces the log p. The presence of surfactant reduces the concentration of drug in oil. Thus, solubility and partition studies indicate that piroxicam may be present at interface. The drug is entering into the palisade layer on the inner side of droplet, which may help to increase the solubility of piroxicam. The partition coefficients were calculated using Eq. 1 (41);

$$P = \frac{A(\text{org}) \times \text{Vf}(\text{org}) \times V(\text{aq})}{A(\text{aq}) \times V(\text{org}) \times \text{Vf}(\text{aq})} \quad (1)$$

where A(org) is the absorbance of the organic layer, A(aq) is the absorbance of the aqueous layer, Vf(org) is the final volume of the sample from the organic layer, V(org) is the volume of the aliquot from the organic layer, Vf(aq) is the final volume of the sample from the aqueous layer, and V(aq) is the volume of the aliquot of the aqueous layer.

Micelle/Buffer Partition Coefficient

Figure 11 shows the differential absorption spectra of drug (piroxicam) in the presence of various concentrations of Tween 80 having constant S/CoS ratio (1:2).

The buffer–micelle partition coefficient K_c ($dm^3\ mol^{-1}$), a useful parameter to quantify the solubilization of piroxicam in micellar media of Tween 80–ethanol system, can be calculated by using Eq. 2 (42).

$$\frac{1}{\Delta A} = \frac{1}{K_c \Delta A_\infty \left(C_a + C_s^{mo}\right)} + \frac{1}{\Delta A_\infty} \quad (2)$$

Here C_a is the drug concentration (1.0×10^{-5} M), C_s^{mo} represents C_s–CMC_o (CMC_o is the CMC of Tween 80 in water, i.e., 11.0 μM), and ΔA_∞ is the differential absorbance at the infinity of C_s. K_c can be obtained through intercept and slope values of the straight line plot of $1/\Delta A$ against $1/(C_a+C_s^{mo})$, as shown in Fig. 12. The value of K_c is given in Table IV.

The dimensionless partition coefficient p is related to K_c as $p=K_c n_w$, where n_w is the number of moles of water per dm^3 (55.5 mol dm^{-3}), and is reported in Table IV. The standard free energy change of the transfer of additive ΔG_p° from bulk water to micelle can be calculated using the following relation (Eq. 3):

$$\Delta G_p^o = -\text{RTlnp} \quad (3)$$

Here T is absolute temperature and R is the gas constant. The value of ΔG_p° for the piroxicam, using p, is reported in Table IV.

High negative value of ΔG_p° indicates the ease of penetration of drug inside the micelles. This is clearly exhibited by the higher values of p and more negative ΔG_p° for piroxicam, as shown in Table IV. Tween 80 is nonionic surfactant, and there is no electrostatic interaction, and the hydrogen bonding between the polyoxyethylene groups of Tween 80 and piroxicam makes the complex (Tween 80–piroxicam) more hydrophobic, which corresponds to high ΔG_p° value.

CONCLUSION

The conductivity and viscosity studies along the dilution line (in phase diagram) depict the structural transition from *w/o* to *o/w* via bicontinuous phase at ~11% Φ_w (wt.% fraction of aqueous phase). Among the eight selected microemulsions, ME was found to be optimum for the incorporation of piroxicam. After the incorporation of the drug, microemulsion remained stable and optically clears, with no phase separation. The drug is entering into the palisade layer on the inner side of the droplet, which may result in controlled release of drug. Thus, we can conclude that this microemulsion system helps in increasing the solubility of a highly hydrophobic drug, with the help of hydrophobic component of microemulsion and lipophilic part of surfactant. In addition, the formulation can be explored with high concentration of drug. Results of conductivity, viscosity, density, and surface tension measurements confirm the prediction of a percolation transition to a bicontinuous structure.

ACKNOWLEDGMENTS

The financial support of Quaid-i-Azam University and Higher Education Commission of Pakistan is duly acknowledged.

REFERENCES

1. Lopes LB, Scarpa MV, Pereira NL, De Oliveira LC, Oliveira AG. Interaction of sodium diclofenac with freeze-dried soya phosphatidylcholine and unilamellar liposomes. Revista Brasileira de Ciencias Farmaceuticas/Brazilian Journal of Pharmaceutical Sciences. 2006;42(4):497–504.
2. Park ES, Cui Y, Yun BJ, Ko IJ, Chi SC. Transdermal delivery of piroxicam using microemulsions. Arch Pharmacal Res. 2005;28 (2):243–8.
3. Yuan Y, Li SM, Mo FK, Zhong DF. Investigation of microemulsion system for transdermal delivery of meloxicam. Int J Pharm. 2006;321(1–2):117–23.
4. Sarciaux JM, Acar L, Sado PA. Using microemulsion formulations for oral drug delivery of therapeutic peptides. Int J Pharm. 1995;120(2):127–36.
5. Ritschel WA. Methods and findings in experimental and clinical pharmacology. 1991;13(3):205–20
6. Mehta SK, Kaur G, Bhasin KK. Analysis of Tween based microemulsion in the presence of TB drug rifampicin. Colloids Surf., B Biointerfaces. 2007;60(1):95–104.
7. Sebastien H, Devin VM, Mark GA, Mark RP. Microfabricated microneedles: a novel approach to transdermal drug delivery. J Pharm Sci. 1998;87(8):922–5.

8. Sintov AC, Botner S. Transdermal drug delivery using microemulsion and aqueous systems: influence of skin storage conditions on the *in vitro* permeability of diclofenac from aqueous vehicle systems. Int J Pharm. 2006;311(1–2):55–62.
9. Spernath A, Aserin A. Microemulsions as carriers for drugs and nutraceuticals. Adv Colloid Interface Sci. 2006;128–130:47–64.
10. Lawrence MJ, Rees GD. Microemulsion-based media as novel drug delivery systems. Adv Drug Deliv Rev. 2000;45(1):89–121.
11. López A, Llinares F, Cortell C, Herráez M. Comparative enhancer effects of Span®20 with Tween®20 and Azone® on the *in vitro* percutaneous penetration of compounds with different lipophilicities. Int J Pharm. 2000;202(1–2):133–40.
12. Fang JY, Yu SY, Wu PC, Huang YB, Tsai YH. *In vitro* skin permeation of estradiol from various proniosome formulations. Int J Pharm. 2001;215(1–2):91–9.
13. Krauel K, Davies NM, Hook S, Rades T. Using different structure types of microemulsions for the preparation of poly (alkylcyanoacrylate) nanoparticles by interfacial polymerization. J Control Release. 2005;106(1–2):76–87.
14. Mehta SK, Kaur G, Bhasin KK. Incorporation of antitubercular drug isoniazid in pharmaceutically accepted microemulsion: effect on microstructure and physical parameters. Pharm Res. 2008;25(1):227–36.
15. He D, Yang C, Ma M, Zhuang L, Chen X, Chen S. Studies of the chemical properties of tri-n-octylamine-secondary octanol-kerosene-HCl-H2O microemulsions and its extraction characteristics for cadmium(II). Colloids Surf A. 2004;232(1):39–47.
16. Podlogar F, Gašperlin M, Tomšič M, Jamnik A, Rogač MB. Structural characterisation of water-Tween 40®/Imwitor 308®-isopropyl myristate microemulsions using different experimental methods. Int J Pharm. 2004;276(1–2):115–28.
17. Sripriya R, Muthu Raja K, Santhosh G, Chandrasekaran M, Noel M. The effect of structure of oil phase, surfactant and co-surfactant on the physicochemical and electrochemical properties of bicontinuous microemulsion. J Colloid Interface Sci. 2007;314(2):712–7.
18. Date AA, Nagarsenker MS. Parenteral microemulsions: an overview. Int J Pharm. 2008;355(1–2):19–30.
19. Pershing LK, Parry GE, Lambert LD. Disparity of *in vitro* and *in vivo* oleic acid-enhanced beta-estradiol percutaneous absorption across human skin. Pharm Res. 1993;10:1745–50.
20. Tanojo H, Junginger HE, Boddé HE. *In vivo* human skin permeability enhancement by oleic acid: transepidermal water loss and Fourier-transform infrared spectroscopy studies. J Control Release. 1997;47(1):31–9.
21. Peltola S, Saarinen-Savolainen P, Kiesvaara J, Suhonen TM, Urtti A. Microemulsions for topical delivery of estradiol. Int J Pharm. 2003;254(2):99–107.
22. Subramanian N, Ray S, Ghosal SK, Bhadra R, Moulik SP. Formulation design of self-microemulsifying drug delivery systems for improved oral bioavailability of celecoxib. Biol Pharm Bull. 2004;27(12):1993–9.
23. Lv FF, Zheng LQ, Tung CH. Phase behavior of the microemulsions and the stability of the chloramphenicol in the microemulsion-based ocular drug delivery system. Int J Pharm. 2005;301(1–2):237–46.
24. Fanun M. Water solubilization in mixed nonionic surfactants microemulsions. J Dispers Sci Technol. 2008;29(8):1043–52.
25. Alany RG, Rades T, Agatonovic-Kustrin S, Davies NM, Tucker IG. Effects of alcohols and diols on the phase behaviour of quaternary systems. Int J Pharm. 2000;196(2):141–5.
26. Kogan A, Garti N. Microemulsions as transdermal drug delivery vehicles. Adv Colloid Interface Sci. 2006;123–126:369–85.
27. Grest GS, Webman I, Safran SA, Bug ALR. Dynamic percolation in microemulsions. Phys Rev A. 1986;33(4):2842.
28. Mehta SK, Bala K. Tween-based microemulsions: a percolation view. Fluid Phase Equilib. 2000;172(2):197–209.
29. Dasilva-Carbalhal J, Garcia-Rio L, Gomez-Diaz D, Mejuto JC, Perez-Lorenzo M. Influence of glymes upon percolative phenomena in AOT-based microemulsions. J Colloid Interface Sci. 2005;292(2):591–4.
30. Podlogar F, Bester Rogac M, Gasperlin M. The effect of internal structure of selected water–Tween 40®–Imwitor 308®–IPM microemulsions on ketoprofene release. Int J Pharm. 2005;302 (1–2):68–77.
31. Kumar P, Mittal KL. Handbook of microemulsion science and technology. Boca Raton: CRC; 1999. p. 357–86.
32. Patzold G, Dawson K. Rheology of self-assembled fluids. J Chem Phys. 1996;104(15):5932–41.
33. Djordjevic L, Primorac M, Stupar M, Krajisnik D. Characterization of caprylocaproyl macrogolglycerides based microemulsion drug delivery vehicles for an amphiphilic drug. Int J Pharm. 2004;271(1–2):11–9.
34. Mitra RK, Paul BK. Physicochemical investigations of microemulsification of eucalyptus oil and water using mixed surfactants (AOT+Brij-35) and butanol. J Colloid Interface Sci. 2005;283 (2):565–77.
35. Leser ME, van Evert WC, Agterol WGM. Phase behaviour of lecithin–water–alcohol–triacylglycerol mixtures. Colloids Surf A. 1996;116(3):293–308.
36. Ding L, Dominska M, Fang Y, Blanchard GJ. Fluorescence and electrochemistry studies of pyrene-functionalized surface adlayers to probe the microenvironment formed by cholesterol. Electrochim Acta. 2008;53(23):6704–13.
37. ZielinÌska K, Wilk KA, Jezierski A, Jesionowski T. Microstructure and structural transition in microemulsions stabilized by aldonamide-type surfactants. J Colloid Interface Sci. 2008;321 (2):408–17.
38. Lianos P. Fluorescence probe study of the interaction between pyrene and microemulsion-polymerized styrene. J Phys Chem. 1982;86(11):1935–7.
39. Kalyanasundaram K, Thomas JK. Environmental effects on vibronic band intensities in pyrene monomer fluorescence and their application in studies of micellar systems. J Am Chem Soc. 1977;99(7):2039–44.
40. Zhang S, Rusling JF. Evaluation of microemulsions of cationic surfactants and a polyoxyethylene cosurfactant for electrolytic dechlorinations of chlorobiphenyls. J Colloid Interface Sci. 1996;182(2):558–63.
41. Songca SP, Mbatha B. Solubilization of meso-tetraphenylporphyrin photosensitizers by substitution with fluorine and with 2, 3-dihydroxy-1-propyloxy groups. J Pharm Pharmacol. 2000;52:1361–7.
42. Khan AM, Shah SS. A UV–visible study of partitioning of pyrene in an anionic surfactant sodium dodecyl sulfate. J Dispers Sci Technol. 2008;29(10):1401–7.